SLAC-PUB-3237
October 1983
(I)

LINEARITY AND RESOLUTION OF PHOTODIODES*

M. A. van Driel† and J. C. Sens†
Stanford Linear Accelerator Center
Stanford University, Stanford, California 94305

ABSTRACT

Measurements are reported of the resolution and linearity of Hamamatsu S1337 Photodiodes mounted on a NaI crystal and exposed to electron energy deposits of up to 80 GeV. The results indicate that these diodes can replace photomultipliers in high-light-yield detectors such as NaI and BGO, when operated in multi-element, compact assemblies in the presence of a magnetic field.

MEASUREMENTS

A 52-cm-long NaI crystal with 150 cm^2 hexagonally shaped cross section was equipped, at one end, with a photomultiplier (AMPEREX X2202B) and with 4 HAMAMATSU S1337 - 1010 BR 1 x 1 cm^2 photodiodes. The setup is shown in Fig. 1. The diodes were connected in parallel to a preamplifier and a Canberra 1410 main amplifier with adjustable time constants for differentiation and integration. The dependence of noise and dark current on detector voltage is shown in Fig. 2. The average energy deposited in the crystal by cosmic rays, signalled by scintillators above and below the crystal (Fig. 1) was 70 MeV. The width of the distribution shown in Fig. 3 is due in part to the spread in angle, in part to the Landau tail.

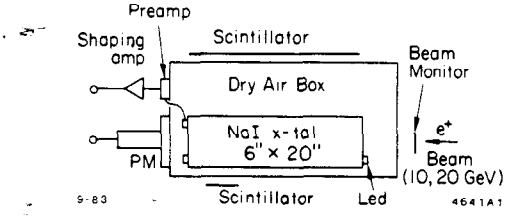

Fig. 1. Assembly of NaI crystal, photomultiplier and photodiode for tests with cosmic rays and LINAC (Beamline 19) positrons at SLAC.

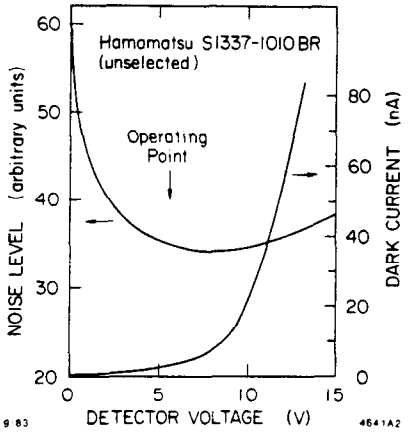

Fig. 2. Noise and dark current versus bias voltage for a S1337 diode.

The purpose of the measurement was to make a comparison, on an event-to-event basis, between the response of a photomultiplier (PM) and a photodiode (PD), when exposed to varying amounts of light. For cosmic ray triggers this comparison is shown in Fig. 4, where the pulseheight seen in the PM and in the PD are compared. For energy deposits up to 700 MeV the relation between PM and PD pulseheights is linear.

In the period November 5-7, 1982, the NaI was placed in Beamline 19 and exposed to positrons of 10 and 20 GeV. The beam was defined with a single scintillator. Operating conditions were LINAC 180 pps, beamline 10 pps. Every 100 msec the beam is gated on for times in the range 0.4-1.4 μsec to permit the passage of RF buckets at the rate of ∿ 3 buckets/nsec. At 1.4 μsec the flux is 9 x 10^9 e^-/mA, converted to 1-2 e^+/mA. Typically, the LINAC current was 300 μA

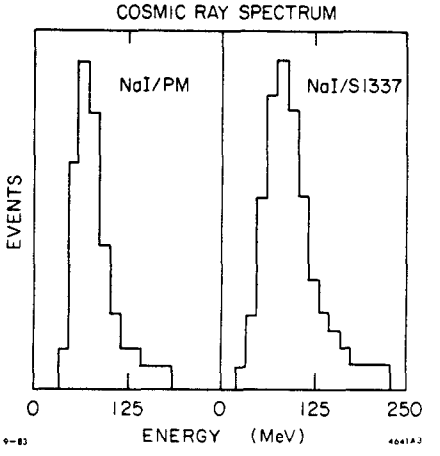

Fig. 3. Spectrum of cosmic rays incident transversely to the NaI axis.

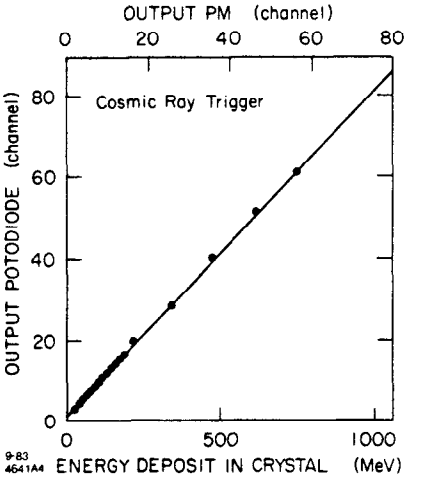

Fig. 4. Comparison of relative linearity of PM and PD response for incident cosmic rays.

At 10 Gev the PD response was optimized by setting the bias voltage at 6V, and the time constants for differentiation and integration to 0.7 and 1.0

*Work supported by the Department of Energy, contract DE-AC03-76SF00515.
†Permanent address: National Institute for Nuclear and High Energy Physics
Amsterdam, The Netherlands

Contributed to the Nuclear Science Symposium, San Francisco, California, October 19-21, 1983.

μsec respectively.

Data were taken with the beamline set for 10 and 20 GeV and for gate lengths of 0.4, 0.8 and 1.4 μsec. For n positrons in the gate, the energy deposited per 100 msec cycle is then n x 10, resp. n x 20 GeV. The number n is Poisson distributed around its mean value $\bar{n}$ which is proportional to the LINAC current.

Fig. 5 shows, event by event, the PM pulseheight versus the PD pulseheight, with the beam set for 10 GeV and $\bar{n}$ approximately equal to 2. Fig. 6 shows the projections on the PM and the PD axes. One observes a discrete spectrum corresponding to n = 1, 2, 3, 4, 5 and 6 positrons per bunch. At each energy 10, 20, 30. . . GeV there is a sharp peak and a lower energy tail.

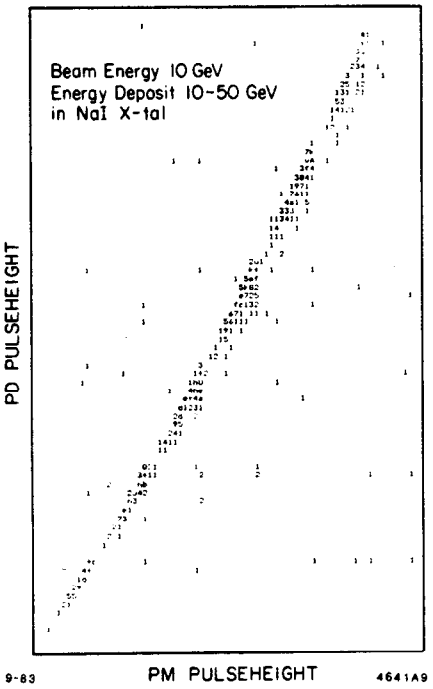

Fig. 5. Comparison of relative linearity of PM and PD response for LINAC positrons. Beamline set to 10 GeV.

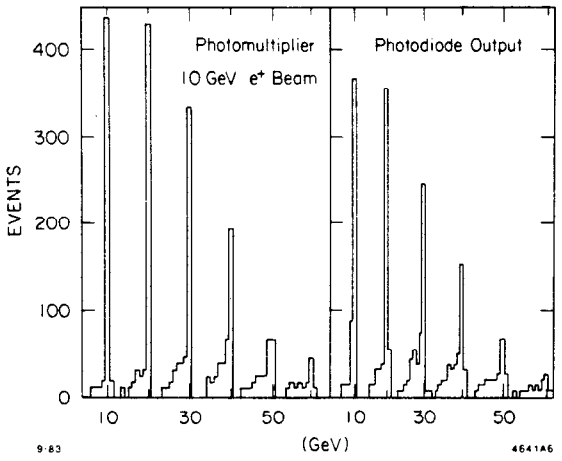

Fig. 6. Projections of the data of Fig. 5

Similar sets of data were obtained for different LINAC currents, different gate lengths and for 20 GeV beam energy. Fig. 7 shows the distribution of positions over the different energies for $\bar{n}$ = 3, in comparison with the expected Poisson distribution. The agreement is good, except at the beam energy (10 GeV), where there is an excess of events.

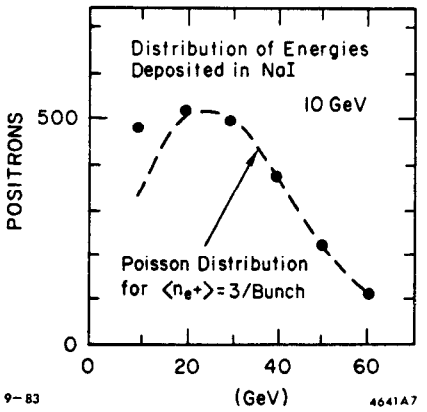

Fig. 7. Distribution of positron intensity over nE, n = 1, 2, 3 . . . , E = 10 GeV, compared with a Poisson distribution for $\bar{n}$ = 3.

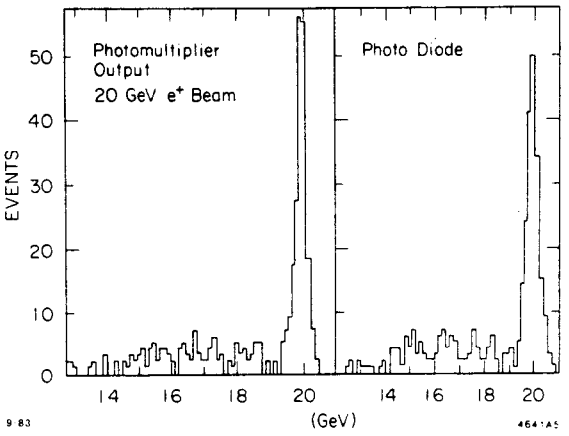

Fig. 8. Comparison of the 20 GeV spectra in the PM and the PD.

Fig. 8 shows, with the beam at 20 GeV, the 20 GeV pulseheight spectra of the PM and the PD with higher gain. Both spectra again show a sharp peak and a lower energy tail. The width of the PD peak is approximately twice that of the PM peak. Fig. 9 shows the width (1 s.d.) of the PD and the PM peaks for n = 1, 2, 3 and 4 corresponding to 20, 40, 60 and 80 GeV for the 20 GeV beam setting. The widths of the PM and PD signals are seen to converge as the energy increases.

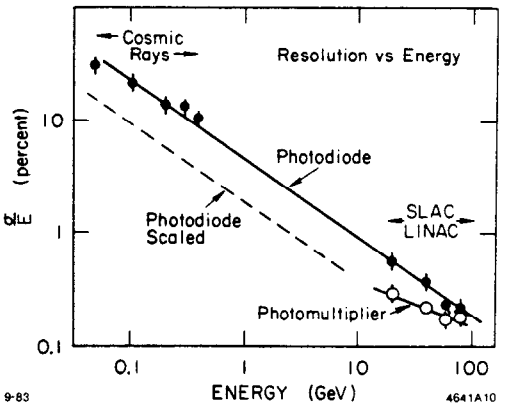

Fig. 9. Resolution (1 s.d.) of the PM and PD versus deposited energy. The dashed curve indicates the resolution the photodiode would have if, for a given energy deposited, the number of e-h pairs would equal the number of photoelectrons produced in the photomultiplier.

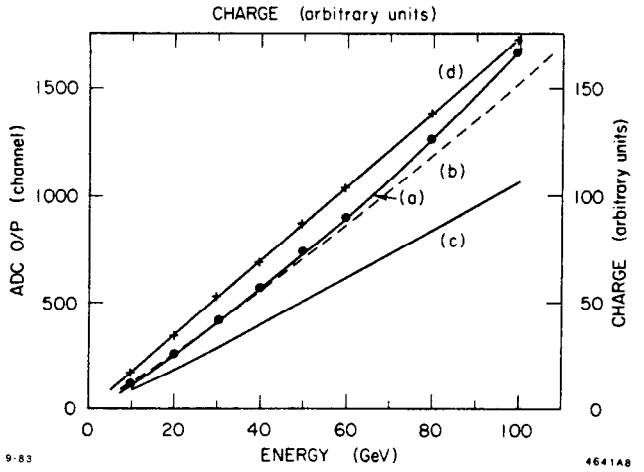

Fig. 10. Response of the S1337 photodiode. o = measured pulseheight (ADC channels) of the PD versus energy deposited in the NaI crystal. Curve (a): best fit to these data. Curve (b): pulseheight output of the preamplifier + amplifier + ADC chain for given amounts of charge injected into the preamplifier. Curve (c), derived from Curves (a) and (b): charge delivered to the preamplifier at various amounts of incident energy. Curve (d): pulseheight (ADC) of the PM versus energy. A fit shows that the PM response is linear. The PM is directly connected to an ADC. +: measured PM data. The curves show that both the PM and PD response is linear, but that the PD electronics is non-linear.

In Fig. 10 we compare the weighted average pulseheights in the PD and the PM for 10, 20, etc., GeV energy deposits in the crystal. This is an extension of the (continuous) cosmic ray data of Fig. 4 towards higher light yields in the PM and PD. We observe that there is approximate linearity and that at higher light yields the average pulseheight of the PD increases faster than that of the PM. Injecting known amounts of charge into the PD preamplifier, we find that most of this increase is due to non-linearity of the electronics. Fig. 10 also shows the relation between the energy deposited in the crystal and the amount of charge delivered by the PD. Here the "electronic" non-linearity has been eliminated and we appear to be left with a linear relation between electron energy and light yield in the PD. At 100 GeV the residual non-linearity is less than 1%.

DISCUSSION

The data obtained in this test show that photomultipliers may be replaced by inexpensive, less bulky, magnetically insensitive photodiodes without serious loss of resolution or linearity up to relatively high energies. An obvious disadvantage is the slowness of the response common to all solid state detectors, and the relatively high noise. This implies the need for preamplifiers and pulseshaping and limits the application to inherently "slow" detectors: NaI, BGO and Pb glass.

At a more quantitative level, some caution is required in interpreting the results of this test. The results are affected by 3 factors:

1. Shower containment calculations indicate that $\sim$ 90% of the energy of a 10 GeV electron is deposited in the 20-rad-length-long, 150 cm^2 NaI crystal.

2. The light reaching the end face either falls on the PM or on the PD's. The end face is covered with reflecting paper with a 10 cm diameter hole to match the PM. Assuming uniform illumination and 100% absorption of the light falling on the PM, the ratio of the area matching factors of the PD's and the PM is 5.4%, see Table I. The PD's are in direct contact with the NaI; the PM views the crystal through $\sim$ 2 cm air, a quartz window, $\sim$ 1/2 cm air and a $\sim$ 15-cm-long light pipe. The optical transmission coefficient has a large uncertainty; from reflections at the different windows we estimate it to be 50%. The NaI spectrum peaks at 410 nm. At 410 nm the ratio of the quantum efficiencies of the PD and the PM is 2.6. The ratio of the number of photoelectrons (p.e.) seen by the PD and the PM is thus 0.27. The effective energy scale applicable to the PD data is thus shifted downwards by this factor.

3. Since shower containment varies non-linearly with energy, the response of the crystal to n showers, each of energy E, differs from that to one shower of energy nE. For example the rear leakage of a 20 GeV shower contained in 20 rad lengths is $\sim$ 1.9%, while that of two 10 GeV showers is 2 x 1.5%. With these caveats we conclude:

   a) From the observed linear relationship between the PM pulseheight and the incident energy (see Fig. 10), it follows that the fraction of the energy deposited in the crystal is independent of energy. The linearity observed in the PD data suggests that the distribution of the light reaching the end fact does not vary significantly with energy.

   b) At a given amount of energy deposited in the crystal, there is an apparent difference in resolution between the PM and the PD spectra. As pointed out in 2. above, this is due to the combined effect of differences in area-matching, optical transmission and in wave length matching (quantum efficiency) between the detector and the NaI crystal. Plotting the data against the number of photoelectrons and electron-hole pairs seen in the PM and the PD respectively, we obtain the dotted line in Fig. 9. We observe that, scaled to equal numbers of photoelectrons (e-h pairs), the PD and the PM curves become roughly continuous suggesting that the resolution is dominated by the p.e and e-h pair statistics and not by systematic effects in the detectors. This conclusion is necessarily somewhat crude, in particular since the optical transmission to the PM is not well-known.

   c) Both the PM and PD spectra show sharp peaks followed by lower energy tails extending over several GeV. Fig. 5 shows that the tails are strongly correlated and are thus not due to differences in response of the detectors or the electronics, but, instead, have their origin in variations in the amount of light deposited in the crystal. The tails become longer at higher energies. A possible source is the combined effect of <100% shower containment and the fact that, e.g. for the 10 GeV beam setting, the total energy deposited is

made up out of n x 10 GeV (n = 1, 2, 3 . .) showers, each with a ∿ 90% probability for full containment.

APPLICATION TO BGO

In LEP3, one of the experiments approved for LEP, an E.M. calorimeter is under consideration consisting of 12000 BGO crystals with photodiode readouts. These crystals will detect electrons and photons with $1 \lesssim E \lesssim 50$ GeV. The size of the crystals is approximately 3 x 3 cm^2 x 20 rad lengths. We assume the entire surface, not covered by PD's, to be reflective; the area-matching factor is then = 1 irrespective of the number and size of the PD's. BGO differs from NaI in that the luminescence is about 25% of that of NaI. Due to the high index of refraction, part of the light is trapped and absorbed. Depending on the optical coupling, the resulting light yield is 8-16% of that of NaI. We assume 12%. The BGO emission spectrum peaks at 480 nm, NaI at 410 nm; PD's are therefore better matched to BGO than to NaI: the quantum efficiency is 72% for BGO, 65% for NaI. The LEP3 BGO crystals have an estimated shower containment of 84%.

The factors entering the comparison are listed in TableI. From the product of the luminescence, shower containment, area and wave length matching factors, we obtain for the relative light yield per unit of incident electron or photon energy:

NaI + PM	1.0
NaI + PD	0.27
BGO + PD	0.68

In terms of light yield and resolution, the results reported here thus bracket the expected performance of the LEP3 BGO detector. Shifting the photodiode curve in Fig. 9 (solid line) to the left by a factor 0.68, one obtains an estimate of the expected LEP3 BGO resolution in the LEP energy range.

After completion of the measurements we learned of a new photodiode, HAMAMATSU S1723, with improved characteristics. Work on this diode, and much of the early work on photodiodes, has been done by D.E. Groom (UU/HEP 83-8, University of Utah).

We would like to thank Roger Gearhart and Ted Fieguth for setting up the beam, and Joost Weber for help with the electronics.

TABLE I

(1)	CRYSTAL	NaI	NaI	BGO
(2)	DETECTOR	PHOTOMULTIPLIER	PHOTODIODE (HAMAMATSU S1337)	PHOTODIODE (HAMAMATSU S1337)
(3)	AREA CRYSTAL (cm^2)	150	150	9
(4)	LENGTH CRYSTAL (R.L)	20	20	20
(5)	NO OF DETECTORS	1	4	2
(6)	EFFECTIVE AREA PER DETECTOR (cm^2)	78.5	1 x 1	1 x 1
(7)	REFLECTING ENDFACE	YES	NO	YES
(8)	AREA MATCHING FACTOR	0.95	0.05	1.0
(9)	RELATIVE LUMINESCENCE	1.0	1.0	0.12
(10)	PEAK EMISSION SPECTRUM (nm)	410	410	480
(11)	OPTICAL TRANSMISSION	0.5	1.0	1.0
(12)	QUANTUM EFFICIENCY AT PEAK	0.25	0.65	0.72
(13)	SHOWER CONTAINMENT	0.90	0.90	0.84
(14)	REL. LIGHT YIELD PER UNIT OF INCIDENT PHOTON OR ELECTRON ENERGY (= (8) x(9) x(11) x(12) x(13))	1.0	0.27	0.68